Acetylcholinesterase: Diffusional Encounter Rate Constants for Dumbbell Models of Ligand

Jan Antosiewicz, Michael K. Gilson, Irwin H. Lee, and J. Andrew McCammon
Department of Chemistry, University of Houston, Houston, Texas 77204-5641 USA

ABSTRACT For some enzymes, virtually every substrate molecule that encounters the entrance to the active site proceeds to reaction, at low substrate concentrations. Such diffusion-limited enzymes display high apparent bimolecular rate constants ((k_{cat}/K_M)), which depend strongly upon solvent viscosity. Some experimental studies provide evidence that acetylcholinesterase falls into this category. Interestingly, the asymmetric charge distribution of acetylcholinesterase, apparent from the crystallographic structure, suggests that its electrostatic field accelerates the encounter of its cationic substrate, acetylcholine, with the entrance to the active site. Here we report simulations of the diffusion of substrate in the electrostatic field of acetylcholinesterase. We find that the field indeed guides the substrate to the mouth of the active site. The computed encounter rate constants depend upon the particular relative geometries of substrate and enzyme that are considered to represent successful encounters. With loose reaction criteria, the computed rates exceed those measured experimentally, but the rate constants vary appropriately with ionic strength. Although more restrictive reaction criteria lower the computed rates, they also lead to unrealistic variation of the rate constants with ionic strength. That these simulations do not agree well with experiment suggests that the simple diffusion model is incomplete. Structural fluctuations in the enzyme or events after the encounter may well contribute to rate limitation.

INTRODUCTION

The enzyme acetylcholinesterase (AChE) terminates transmission at cholinergic synapses by hydrolysing acetylcholine (ACh) into acetic acid and choline (Stryer, 1981; Barnard, 1974). AChE is an extremely effective catalyst, acting on its natural substrate at rates in the range customarily associated with diffusion-controlled reactions (Fersht, 1985). That the effective bimolecular rate constant ((k_{cat}/K_M)) falls with increasing solvent viscosity (Bazelyansky et al., 1986) supports the idea that AChE is diffusion controlled, and the decline of (k_{cat}/K_M) with ionic strength (Berman et al., 1991) also suggests that the encounter of the cationic substrate with its negatively charged enzyme is at least partly rate limiting.

The kinetics of encounter of a substrate with its enzyme may be explored by means of Brownian dynamics simulations of a substrate diffusing in the neighborhood of the enzyme (Ermak and McCammon, 1978; McCammon et al., 1986; Davis et al., 1991; Wade et al., 1994). In a previous study, we used such simulations to compute the effective bimolecular rate constants for the encounter of *Torpedo californica* AChE with its substrate, as a function of ionic strength (Antosiewicz et al., 1994a). The results suggested that translational electrostatic steering of ligands indeed contributes to the large bimolecular rate constants of the enzyme. In addition, the observed fall in rate constant with increasing ionic strength was qualitatively reproduced. However, the slope of the rate constants with increasing ionic strength was larger than observed experimentally, and the absolute rate constants for enzyme-ligand encounter considerably exceeded measured rate constants for hydrolysis of acetylthiocholine (ATCh) and for fluorescence quenching of *N*-methylacridinium (NMA). We hypothesized that much of the inaccuracy resulted from the inadequacy of the assumption that any substrate molecule that reaches the entry to the active site of AChE proceeds to reaction.

The present paper describes our efforts to improve this aspect of the model through the use of a somewhat more detailed criterion for the encounter of the ligand with the enzyme. In particular, we consider the possibility that imposing an orientational criterion for the encounter, in addition to the translational criterion, may bring the computed results into better agreement with the measured data. The idea is that the computed encounter rates are overestimated partly because the probability that substrate will react (or that NMA will be quenched) is low when the ligand arrives with its long axis oriented at an angle to the long axis of the active site gorge. Also, for a ligand such as ACh or ATCh that has an electrical dipole moment, the rate constants and their dependence upon ionic strength could reflect orientational as well as translational steering effects. In analogous simulations of the encounter of the enzyme triose phosphate isomerase (TIM) with its substrate glyceraldehyde phosphate, it has been found that the computed rate constants are more accurate when the simple single-bead substrate model is replaced by a structured substrate model, together with an orientational encounter criterion (Luty et al., 1993b; Wade et al., 1994).

Received for publication 17 June 1994 and in final form 30 September 1994.

Address reprint requests to Dr. J. Andrew McCammon, Departments of Chemistry and Biochemistry and Pharmacology, University of California at San Diego, La Jolla, CA 92093-0365. E-mail: jmccammon@ucsd.edu.

Dr. Antosiewicz is on leave from the Department of Biophysics, University of Warsaw, 02-089 Warsaw, Poland.

Dr. Gilson's current address: Center for Advanced Research in Biotechnology, 9600 Gudelsky Dr., Rockville, MD 20850-3479.

I. H. Lee was on summer leave from Harvard College.

0006-3495/95/01/62/07 $2.00

We therefore carry out simulations of AChE with a dumbbell-shaped ligand, consisting of two spheres, the diffusion properties and charge distribution of which approximate those of ACh. Other refinements include the use of a more realistic dielectric model of the enzyme and a more careful estimate of the relative diffusion coefficient of the ligand and enzyme.

The main effect of using the dumbbell model with an orientational reaction criterion is a significant drop in the resulting calculated rate constants relative to those for the single-bead ligand. The agreement with experiment is therefore improved in this respect. However, the slope of the ionic strength dependence of the rate constant is larger in magnitude than before and therefore deviates more from experiment. We thus argue that accurate calculations of the rate constants will require a more detailed treatment of the events after the encounter of substrate with the active site entry.

MATERIALS AND METHODS

Our procedure for estimating the diffusional encounter rate constants for this enzyme-ligand system has been detailed in the previous work (Antosiewicz et al., 1994a). Here we summarize this procedure and describe in detail the modifications introduced. All electrostatic and Brownian dynamics (BD) calculations are carried out with the UHBD software package (Davis et al., 1991; Madura et al., 1994).

The rate constants of enzyme-ligand encounter are calculated from large numbers of Brownian trajectories of the ligand in the neighborhood of the enzyme (Ermak and McCammon, 1978; McCammon et al., 1986; Wade et al., 1994; Madura et al., 1994). The ligand moves under the influence of the electrostatic field of the enzyme and the random bombardment of solvent molecules. Trajectories are initiated on the surface of a sphere of radius b, the b-surface, around the center of coordinates of the enzyme. This sphere is made sufficiently large so that the electrostatic forces between the ligand and the enzyme are approximately centrosymmetric for $r > b$. Each trajectory is continued until the ligand satisfies a predefined encounter criterion or reaches an outer spherical surface of radius q, the quit-surface. The fraction of trajectories that finish with encounters is corrected to include the additional encounters that would have occurred if the trajectories had not been truncated at the quit-surface and is then multiplied by the rate constant for the encounter of ligand with the b-surface to yield the bimolecular diffusion-controlled rate constant k (Davis et al., 1991). It should be noted that the simulations assume an absorbing boundary condition at the entry to the enzyme active site; the validity of this assumption is considered in the Discussion.

Diffusion coefficient of the ligand

The generation of a Brownian dynamics trajectory requires that the relative translational diffusion coefficient of the enzyme and the ligand be specified. This is the sum of their individual mean translational diffusion constants when hydrodynamic interactions between the enzyme and the substrate are neglected, as is done here (Ermak and McCammon, 1978). Because the ligand is very small relative to the enzyme, its contribution to their relative diffusion coefficient dominates. We have therefore not sought to refine the already detailed diffusion model of the enzyme monomer (Antosiewicz et al., 1994a). However, in our previous study (Antosiewicz et al., 1994a), the ligand was assigned the diffusion constant appropriate to a single sphere of radius 5 Å (stick boundary conditions), based upon the classical Einstein equation (Einstein, 1905) $D = (kT/6\pi\eta r)$, where D is the diffusion constant, k is Boltzmann's constant, T is absolute temperature, η is viscosity, and r is the radius of the sphere. In the present work, we use the following more accurate method to estimate the diffusion constant of the ligand.

The approach is similar to that used for the enzyme (Antosiewicz et al., 1994a). We represent all atoms of the ligand, including hydrogens, as spheres of uniform radius and use a bead model (Garcia de la Torre and Bloomfield, 1981; Antosiewicz and Porschke, 1988) to compute the diffusion coefficient tensor for the entire molecule. The bead radius is selected to optimize the agreement between computed and measured average translational diffusion coefficients for the reference molecules glycine and sucrose. When we assume a planar configuration for the amide group of glycine, and a chair conformation for sucrose, we find the optimal bead radius to be 1.2 ± 0.05 Å. When used with the bead diffusion model, this radius yields average translational diffusion coefficients of 88.4×10^{-7} cm^2s^{-1} and 49.5×10^{-7} cm^2s^{-1} for glycine and sucrose, respectively. The corresponding experimental values, at 293 K, are 93.3×10^{-7} cm^2s^{-1}, and 45.9×10^{-7} cm^2s^{-1} (Cantor and Schimmel, 1980), so the level of agreement appears to be satisfactory. We use this 1.2-Å radius with the bead model and an assumed all-trans molecular conformation to estimate an average translational diffusion constant for ACh of 61.7×10^{-7} cm^2s^{-1}. A similar result is obtained when the average structure from a molecular dynamics simulation of ACh (I. Lee et al., unpublished results) is considered.

We obtain similar values (57.1×10^{-7} cm^2s^{-1} and 59.7×10^{-7} cm^2s^{-1}, respectively) for the AChE inhibitors tacrine (9-amino-1,2,3,4-tetrahydroacridine) (Pop et al., 1989) and NMA. These values are all close to that appropriate to a 3.5-Å sphere (see formula above), 61.2×10^{-7} cm^2s^{-1}, and this is the value used in all of the calculations in the present paper. However, because we previously assumed an effective ligand radius of 5 Å (Antosiewicz et al., 1994a), the diffusion constant used here is significantly larger. It is also worth remarking that when these calculations of diffusion constant are carried out without including hydrogen atoms explicitly for glycine, sucrose, ACh, tacrine, and NMA, the changes in the results are negligible.

Simulation models of the ligand

The present study considers both single-bead and dumbbell models of the ligand. Based upon the preceding analysis, the single-bead model is assigned the diffusion coefficient appropriate to a sphere of radius 3.5 Å (stick boundary conditions). To investigate the effects of the electrostatic field of the enzyme on its diffusional encounter with the single-bead ligand, we consider both the case in which the ligand has the +1 e charge appropriate for ACh, tacrine, and NMA (model A) and that in which the single-bead ligand is uncharged (model B).

The dumbbell model of the ligand is based upon ACh. It consists of two spheres of equal size and separated by 4.63 Å, which is the distance between the centers of coordinates of the choline moiety (CH_2-$N(CH_3)_3$) and the ester moiety (CH_3-CO-O-CH_2) of ACh in the all-trans conformation and, to a good approximation, in the conformations observed in the molecular dynamics simulation of ACh. The bead radii are set to yield an average translational diffusion constant for the entire dumbbell equal to that of a 3.5-Å sphere. When hydrodynamic interactions (Garcia de la Torre and Bloomfield, 1981) between the two beads are included during the BD calculations, the appropriate radius is 2.8 Å, and the eigenvalues of the resulting diffusion tensor are $(58.7, 58.7, 64.6) \times 10^{-7}$ cm^2s^{-1}. In one calculation (see below), hydrodynamic interactions between the two beads are neglected, leading to an isotropic translational diffusion tensor. In this case, setting the bead radii to 1.75 Å yields the desired overall diffusion constant.

For the dumbbell models, the charge of each bead is just the total of the atomic charges for the corresponding chemical moiety, where the partial charges are taken from CHARMm version 22.0 (Brooks et al., 1982; Molecular Simulations Inc., 1992). This results in a charge of 0.79 e for the choline bead and 0.21 e for the ester bead.

We consider several variations of the dumbbell model. As detailed below, the reaction criteria for the dumbbell models involve establishing one of the beads as reactive. That is, a trajectory is said to end in reaction (or, more properly here, in encounter) when the reactive bead enters the mouth of the active site gorge. In models C and D, the beads corresponding to the choline and ester moieties respectively are defined as reactive. In model E, both beads are set electrically neutral and one is arbitrarily made reactive. In model F, the charges are included and the choline bead defined as reactive,

but hydrodynamic interactions between the two beads are neglected, resulting in an isotropic diffusion tensor. Comparisons of the computed encounter rate constants for these various models yield information about the influence of translational and orientational steering and of diffusional anisotropy for charged ligands interacting with AChE.

Electrostatic potential around AChE

Calculating the electrostatic potential in the aqueous medium around the enzyme requires two steps. The first is the calculation of the average charge of each ionizable group of the enzyme for the selected pH and ionic strength. The second is the use of these charges in the computation of the average electrostatic field in which the ligand will diffuse.

The procedure for calculating the average charges of the ionizable groups (Antosiewicz et al., 1994a; Antosiewicz et al., 1994b) is described only briefly here. The finite difference Poisson-Boltzmann method is used to calculate self energies and interaction energies of ionizable groups for each ionic strength. These energies are used to calculate the mean charges of the ionizable groups at pH 7.0, which is the value at which the experimental data quoted in this work were obtained. The cluster (Gilson, 1993) method is used to treat the multiple site titration problem. Partial charges for the neutral forms of the amino acids, required for these calculations, are taken from CHARMm Version 22.0 (polar hydrogen only parameter set) (Brooks et al., 1982; Molecular Simulations Inc., 1992). The radius of each atom type i is set to $0.5\sigma_i$, where σ_i is the appropriate van der Waals radius parameter of the OPLS nonbonded parameter set (Jorgensen and Tirado-Rives, 1988). Histidine tautomer assignments are the same as used previously (Antosiewicz et al., 1994a). The temperature is set at 300°K, and the solvent dielectric constant to 78.0, with ionic strengths of 20, 150, or 500 mM. The dielectric constant of the protein interior is set at 15. This deviates slightly from the value of 20 which has been shown to yield pKas in excellent agreement with experiment (Antosiewicz et al., 1994b). However, when repeated with a protein dielectric constant of 15, the titration calculations of reference (Antosiewicz et al., 1994b) yield pKas that agree with experiment as well, overall, as those calculated with a protein dielectric constant of 20 (J. Antosiewicz, unpublished results). The dielectric boundary between protein and solvent is defined as a Richards probe-accessible surface (Richards, 1977), with a 1.4-Å probe radius, and an initial set of 280 surface dots per atom (Gilson et al., 1988).

Note that in our previous study, the dielectric boundary was defined as a van der Waals surface, and the protein dielectric constant was set at 4. Although a rather different dielectric model is used here, it turns out that the resulting predicted pKas are similar. This is because, with the van der Waals surface definition, high dielectric solvent fills the cracks and crevices between the atoms of the protein. This causes the protein as a whole to have a rather high effective dielectric constant. Indeed, the total protein charges computed here agree well with those computed previously (Antosiewicz et al., 1994a).

As previously described (Antosiewicz et al., 1994a), for each ionizable residue the average charge computed for pH 7.0 and the desired ionic strength is added to the partial charge of the ionization site (Antosiewicz et al., 1994b) of the neutral form of the amino acid. Nonionizable residues are also assigned partial charges from the CHARMm 22.0 polar hydrogen parameter set (Brooks et al., 1982; Molecular Simulations Inc., 1992) to yield a complete set of atomic charges for the protein under the selected solution conditions for use in computing the electrostatic field around the enzyme.

The field calculations use the same atomic and molecular parameters as the ionization calculations, except that a protein dielectric constant of 4 is assumed. This lower value makes sense theoretically, because for a given charge state and conformation of the enzyme, orientational polarizability should be unimportant in calculating the field (Gilson and Honig, 1986). Furthermore, BD calculations on the enzyme superoxide dismutase yielded optimal agreement with experimentally measured rates when a low protein dielectric constant was used in computing the electrostatic field (Klapper et al., 1986). In the present work, the finite difference calculations of the field around the enzyme use a grid spacing of 1.0 Å. At 20 mM ionic strength, at which a strong field extends far from the enzyme, a 130 × 130 × 130 grid is used. At 150 mM and 500 mM ionic strength, at which the weaker field permits the use of a less extensive grid, a 110 × 110 × 110 grid is used. At 20 mM, the electrostatic potential at the border of the 130-Å grid is greater than that at the border of the 110-Å grid at 150 mM and 500 mM but is still several times less than kT/e.

Brownian dynamics simulations

As described above, we carry out BD simulations for both single-bead and dumbbell models of the ligand. For the former, we use reaction criteria identical to those used in our previous study (Antosiewicz et al., 1994a). That is, we define the axis of the active site gorge as the line connecting CD of Ile 444 (the bottom of the gorge) with a point at the average coordinates of Glu 73 CA, Asn 280 CB, Asp 285 CG, and Leu 333 O (the gorge entry). The reaction center for the single-bead ligand is defined as a point on the axis 2 Å further into the gorge than the gorge entry. Encounter is said to occur when the single-bead ligand approaches to some distance of this reaction center. Distances of 1, 3, 5, and 7 Å are considered.

The reaction criteria for the dumbbell model of the ligand include an orientational restriction. This is implemented by defining a second reaction center on the gorge axis 4.63 Å (the distance between the dumbbell beads) farther out than the first reaction center. Encounter is said to occur when the reactive bead (see above) comes within some distance of the first reaction center and the other bead simultaneously comes within the same distance of the second reaction center. Again, distances of 1, 3, 5, and 7 Å are considered. It should be noted that the larger distances imply not only a less restrictive positional criterion but also a less restrictive orientational criterion, as diagrammed in Fig. 1.

The b sphere radii used in generating the BD trajectories are 55.0 Å at 150 and 500 mM ionic strength and 65.0 Å at 20 mM. In all calculations, the q sphere radius is set to 300 Å. This is half the radius used previously, but test calculations demonstrated that the change does not affect the computed rate constants. Steric exclusion of the ligand by the enzyme is accounted for by prohibiting any ligand bead center from coming closer than 3 Å to the van der Waals surface of any protein atom.

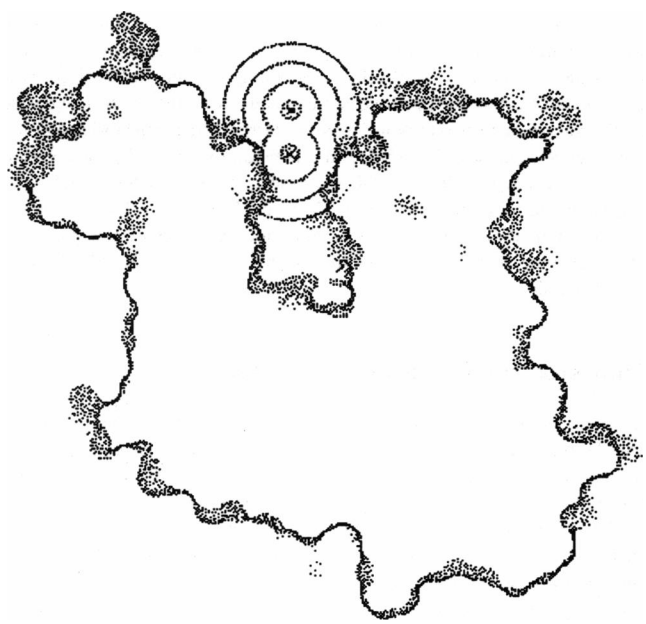

FIGURE 1 Cross-section of the solvent-accessible surface of AChE, showing the two reaction centers in the mouth of the active site gorge, along with the 1-, 3-, 5-, and 7-Å spherical zones used in defining the reaction criteria. The inner reaction center is used for the single-bead models and for the reactive bead of the dumbbell models. The outer reaction center is used for the nonreactive bead of the dumbbell models.

We use the same variable time steps as in the previous study (Antosiewicz et al., 1994a). When the ligand is closer than 40 Å to the center of the AChE monomer, the time step is set to 0.02 ps. Between 40 and 100 Å the time step is 0.2 ps, and beyond 100 Å, the time step is 2.0 ps. The validity of these choices has been discussed (Antosiewicz et al., 1994a). Except for one calculation noted in the text, every BD simulation comprises 5000 separate trajectories.

RESULTS

Comparisons among the models

Results for various models of the ligand are compared in Table 1, which presents the computed rate constants at pH 7.0 and 150 mM ionic strength for ligand models A-F, and for reaction criteria based upon distances of 1–7 Å.

The results for the single-bead models support the previous observation (Antosiewicz et al., 1994a) that the electrostatic field of the enzyme results in a significant increase in the encounter rate. Thus, the ratios of the encounter rate constants of the charged to the neutral single-bead ligand are 3.9, 5.4, 9.4, and 22.6 for the 7-, 5-, 3-, and 1-Å reaction criteria, respectively. The corresponding ratios from our previous study are 3.4, 4.7, 7.0, and 12. The modest difference between these two sets of ratios appears to result from the somewhat stronger electrostatic field calculated here. This in turn results from the different dielectric model of the protein. Previously, the field around the enzyme was computed with a van der Waals model for the protein surface and a protein dielectric constant of 4. Here, although the same protein dielectric constant was used, the dielectric boundary is defined as a Richards probe-accessible surface. As a consequence, the average dielectric constant of the protein is lower and the field of the enzyme stronger. Note also that, as shown in Table 1, the computed encounter rates for the neutral, single-bead ligand are somewhat greater here than before (Antosiewicz et al., 1994a). This is a consequence of the greater diffusion constant assigned to the ligand (see Materials and Methods).

For the dumbbell models, we observe some orientational preference in the encounter of the charged models, the rate constant for the dumbbell oriented with the more positively charged choline bead pointing into the gorge entry (i.e., reactive choline, model C) is greater than that for the encounter with the ester group pointing inward (reactive ester, model D). This effect is very modest for the 7-Å reaction criterion (ratio 1.3) and somewhat greater for the more orientationally restrictive 1-Å reaction criterion (ratio 2.3). The statistical uncertainties are rather large compared with the differences, but the comparison consistently favors the reactive choline model. This orienting effect of the field is superimposed upon a much greater translational effect. That is, although the electrostatic field does favor one particular orientation of the dumbbell ligand, it accelerates encounter with the substrate in either orientation relative to the case of a neutral dumbbell. Furthermore, comparison of the rate constants for the charged dumbbell models C and D with the results for the neutral model E shows that the electrostatic field actually has a greater steering effect on the dumbbell ligands than on the single-bead ligands. For example, the ratio of the rate constant for model C to that of model E, for the 3-Å reaction criterion, is 16.7, greater than the corresponding ratio of 9.4 for models A and B.

When hydrodynamic interactions between the two beads of the dumbbell ligand are accounted for, as they are in all the dumbbell models except F, the translational diffusion tensor of the ligand is anisotropic. That is, the ligand diffuses longitudinally more readily than it does laterally. Comparison of models C and F, two dumbbell models that differ only in whether they include hydrodynamic interactions between the beads, shows that any effect of this diffusional anisotropy upon the encounter rates is negligible in this system.

Table 2 presents the dependence upon ionic strength of the computed rate constants for two ligand models: the charged single-bead (model A) and the charged dumbbell with the choline bead reactive (model C). These data are also presented graphically in Fig. 2. As shown, the rate constants for the dumbbell model are smaller than those for the single-bead model at every ionic strength and for each encounter radius (7, 5, 3, and 1 Å). This result is not surprising, given that the dumbbell model of the ligand is sterically larger than the single-bead ligand and that more restrictive reaction criteria are applied to it.

What is more interesting is that the encounter rates for the dumbbell model fall off more rapidly with increasing ionic strength than do those for the single-bead model, particularly

TABLE 1 Calculated rate constants (units 10^9 M^{-1} s^{-1}; ±90% confidence limits) for AChE monomer and various models of the ligand at 300 K, pH 7, 150 mM ionic strength

Model of ligand	Reaction distance from dummy atom			
	7Å	5Å	3Å	1Å
A: Charged single bead	3.70 ± 0.26	2.97 ± 0.24	2.45 ± 0.22	1.81 ± 0.19
B: Neutral single bead	0.94 ± 0.14	0.55 ± 0.11	0.26 ± 0.07	0.08 ± 0.04
C: Charged dumbbell, choline reactive	2.69 ± 0.23	1.95 ± 0.20	1.03 ± 0.15	0.21 ± 0.08
D: Charged dumbbell, ester reactive	2.11 ± 0.20	1.56 ± 0.18	0.67 ± 0.12	0.09 ± 0.04
E: Neutral dumbbell	0.67 ± 0.12	0.31 ± 0.08	0.06 ± 0.04	NR
F: Charged dumbbell, choline reactive; no hydrodynamic bead-bead interaction	2.54 ± 0.22	1.97 ± 0.20	1.22 ± 0.16	0.25 ± 0.08
Previous results, charged single bead	2.41 ± 0.17	1.86 ± 0.15	1.39 ± 0.13	0.84 ± 0.10
Previous results, neutral single bead	0.71 ± 0.06	0.40 ± 0.05	0.20 ± 0.03	0.07 ± 0.02

See text for definitions of models. For comparison, the last two lines provide previous results (Antosiewicz et al., 1994a). NR, no reaction occurred

TABLE 2 Calculated rate constants (10^9 M^{-1} s^{-1}; ± 90% confidence limits) for encounter of the AChE monomer with ligand for the charged single-bead model (model A) and the charged dumbbell with reactive choline (model C)

Ligand	I (mM)	q (e)	Reaction distance criterion			
			7 Å	5 Å	3 Å	1 Å
Charged single bead	20	−5.3	9.10 ± 0.35	8.47 ± 0.35	7.69 ± 0.34	6.30 ± 0.32
	150	−6.1	3.70 ± 0.26	2.97 ± 0.24	2.45 ± 0.22	1.81 ± 0.19
	500	−6.5	1.87 ± 0.19	1.32 ± 0.16	0.80 ± 0.13	0.51 ± 0.10
Charged dumbbell with choline reactive	20	−5.3	7.50 ± 0.38	6.56 ± 0.37	4.91 ± 0.33	1.31 ± 0.18
	150	−6.1	2.69 ± 0.23	1.95 ± 0.20	1.03 ± 0.15	0.21 ± 0.08
	500	−6.5	1.49 ± 0.17	0.92 ± 0.14	0.39 ± 0.09	0.05 ± 0.03

Results are for 300°K, pH 7, and listed ionic strengths (I). q, net charge of the protein

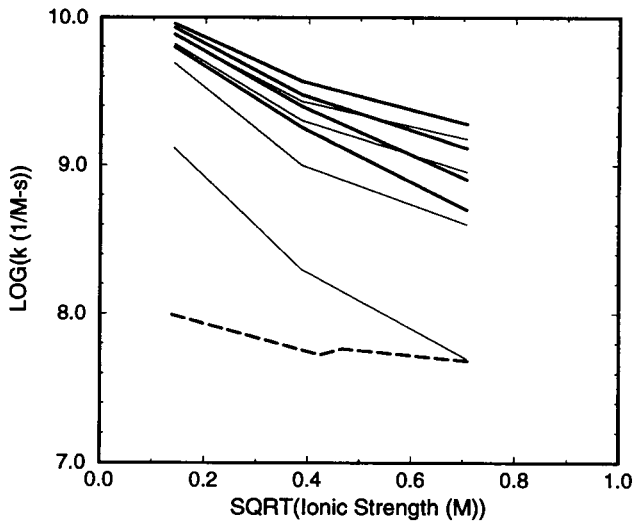

FIGURE 2 Comparison of calculated encounter rate constants and experimental hydrolysis rate constants k (M^{-1} s^{-1}) versus ionic strength I (M) for monomeric and dumbbell models of the ligand. *Thick solid lines*: monomer model A, for 7-, 5-, 3-, and 1-Å encounter criteria. *Thin solid lines*: dumbbell model C, for 7-, 5-, 3-, and 1-Å encounter criteria. (Larger encounter radii are associated with higher rates.) *Dashed line*: experimental rate constants for hydrolysis of ATCh (Berman et al., 1991; Radić et al., 1992). See Tables 2 and 3 for data.

for the more restrictive reaction criteria, 1 and 3 Å. We initially supposed that this increased dependence upon ionic strength resulted from the fact that the electrostatic field provides both translational and orientational steering for this ligand model. However, this does not appear to be the correct explanation. If it were, rate constants for the dumbbell ligand with the ester bead reactive (model D), for which orientational steering should oppose the encounter, should have a weaker ionic strength dependence than the monomer model. Yet a test calculation with model D at 20 mM ionic strength, with 2000 trajectories, showed an ionic strength dependence similar to that for model C. Therefore, the increased dependence of the rate constants for the dumbbell models upon ionic strength does not appear to result from orientational steering. Rather, examination of the results for the single-bead ligand model supports the idea that simply imposing increasingly restrictive encounter criteria increases the dependence of the rate constants upon ionic strength.

Comparison with experimental data

Comparisons of our computed rate constants with measured rate constants for the hydrolysis of ATCh (Berman et al., 1991; Radić et al., 1992) by *Torpedo californica* AChE (Tables 2 and 3; Fig. 2) show that the computed rate constants for the single-bead ligand model substantially overshoot the measured rate constants, regardless of the particular encounter criterion used. Although the rate constants for the dumbbell models are lower, they still exceed the measured values substantially for all but one simulation. Moreover, the reduced absolute rate constants for the dumbbell model are associated with greatly increased dependence of the rate constants upon ionic strength. This strong dependence upon ionic strength disagrees markedly with the experimental data.

DISCUSSION

The very high measured values of (k_{cat}/K_M), and their dependence upon the viscosity and the ionic strength of the solvent, suggest that AChE is a diffusion-controlled enzyme and that electrostatic steering of the substrate contributes to its high catalytic rate. However, previous Brownian dynamics calculations of the encounter of the enzyme with its substrate yielded encounter rate constants considerably larger than the experimental rate constants for hydrolysis of ATCh. The dependence of the rate constants upon ionic strength was also overestimated (Antosiewicz et al., 1994a). The present study seeks to improve the agreement between theory and experiment, primarily through the use of a somewhat more sophisticated treatment of the ligand and the criteria for encounter, although the model is enhanced in several other respects as well.

TABLE 3 Measured effective bimolecular rate constants (k_{cat}/K_m) for hydrolysis (10^9 M^{-1} s^{-1}) of ATCh by the AChE monomer, as a function of ionic strength (mM), at pH 7.0.

Ionic strength	Reference	k_{cat}/K_M
19	Berman et al., 1991	0.098
179*	Radić et al., 1992	0.053
218	Berman et al., 1991	0.058
517	Berman et al., 1991	0.048

*Ionic strength computed for 100 mM phosphate buffer at pH 7.0.

The results confirm the previous finding that the electrostatic field produced by AChE increases the rate constant for its encounter with the cationic substrate. The results also agree qualitatively with the experimental observation that increasing ionic strength reduces the rate constants. Finally, the encounter rate constants for the dumbbell ligands are indeed lower than those for the single-bead models. This drop in rate constant was expected, for two reasons. First, the dumbbell ligand is larger than the single-bead ligand, so it succeeds in entering the active site entry less often. (Note, however, that the average translational diffusion constants are the same for both types of ligand model.) Second, the dumbbell models are used with more restrictive encounter criteria, which require not only that the reactive bead approach the active site to within a specified distance but also that the dumbbell possess the correct orientation relative to the long axis of the active site gorge. Still, the rate constants for the dumbbell ligands as well as for the single-bead ligands exceed the measured rate constants in all but one calculation (see Fig. 2).

It would certainly be possible to devise still more restrictive encounter criteria in an attempt to bring the computed rate constants into agreement with the measured values. However, the results summarized in Fig. 2 show that the use of increasingly restrictive encounter criteria leads to an increasingly unrealistic dependence of the rate constants upon the ionic strength. This holds for both the single-bead and dumbbell models of the ligand. Thus, it appears that the disagreement with experiment does not result simply from the use of excessively loose encounter criteria. How, then, to account for the discrepancies between the computed and measured rate constants?

One possibility is that the strength of the attractive electrostatic field is overestimated. This would result in excessively large rate constants and an excessive decline in the rate constants with ionic strength, as observed. Field overestimates could result from errors in the computed average charges of the ionizable groups of the enzyme. However, the procedure used here has been shown to yield rather accurate predictions of pKa in a number of globular proteins (Antosiewicz et al., 1994b). One way to examine this possibility further would be to repeat the simulations for a significantly lower assumed pH. If the excessive dependence of rate constants upon ionic strength persists despite an artificial and substantial decrease in the negative charge of the enzyme, it will be unlikely that incorrect charge states are responsible for the discrepancy. Field overestimates could also result from the use of an excessively low value for the dielectric constant of the protein. However, this too seems unlikely, because low values such as used here have been shown to yield excellent agreement with experiment in similar calculations on superoxide dismutase (Klapper et al., 1986; Sines et al., 1990) and TIM (Luty et al., 1993b).

Another possible explanation for the overestimates in the computed rate constants is that the simulations neglect two repulsive forces expected to act between the ligand and the enzyme. One results from hydrodynamic interactions between the ligand and the enzyme and the other from desolvation of the cationic ligand as it approaches the enzyme. Inclusion of these effects would reduce the probability of satisfying the encounter criteria and thus lower the computed rate constants. Also, because the ligand would tend to stay a little further from the active site entry, in regions of weaker field, it might reduce the dependence of the rate constants upon ionic strength. On the other hand, simulations of the encounter of superoxide with superoxide dismutase and of glyceraldehyde phosphate with TIM, with similar methods, yielded good agreement with experiment despite the neglect of desolvation forces and hydrodynamic interactions, so it is difficult to understand why this type of adjustment should be needed in modeling the present system.

On the basis of these arguments, we suspect that the encounter rate constants computed here are probably fairly accurate and that most of the error in the present model results from the assumption that every substrate that satisfies the reaction criterion, defined for a rigid model of the enzyme, will proceed to reaction. Although this simple absorbing boundary type of model has been quite successful in models of superoxide dismutase (Klapper et al., 1986; Sines et al., 1990) and TIM (Luty et al., 1993b), it is reasonable that the case of AChE should be different, because its active site is much less accessible. In fact, as determined crystallographically, the active site gorge is too narrow to admit substrate. Nonetheless, AChE inhibitors of the same size as the substrate can diffuse to the bottom of the active site near the catalytic residues in crystalline AChE (Harel et al., 1993). This strongly suggests that conformational fluctuations of the active site gorge are critical for the entry of substrate and points to a complicated and intriguing series of events after the encounter of a molecule of substrate with the active site entry, leading either to its hydrolysis at the bottom of the active site gorge or to its escape. Support for this explanation is in fact emerging from extended Brownian dynamics simulations that make some allowance for fluctuations in the width of the channel to the active site (J. Antosiewicz et al., in preparation). Moreover, although the effects of viscosity and ionic strength upon the measured rate constant for hydrolysis may result primarily from their influence on the initial encounter of enzyme and ligand, it is also possible that these parameters influence events subsequent to the encounter. Thus, suggestively, it has been shown that k_{cat} rises with increasing ionic strength (Berman et al., 1991). Furthermore, if substantial conformational fluctuations are involved in the passage of substrate through the active site gorge, the process of entry may well be affected by the viscosity of the solvent. Finally, chemical steps may also be at least partly rate limiting. The degree to which this is the case is expected to depend upon pH and other solution conditions.

We are currently using molecular dynamics simulations to examine conformational fluctuations of the active site gorge of AChE (Gilson et al., 1994). Ultimately, it should be possible to create a hybrid model of the enzyme-ligand interaction by using Brownian dynamics to treat the initial approach of the ligand to the active site entry and more detailed

molecular dynamics simulations for events subsequent to the encounter (Luty et al., 1993a).

We thank Professor Joel Sussman for providing the coordinates of AChE and helpful advice.

This work was supported in part by the National Institutes of Health, the Robert Welch Foundation, and the Metacenter Program of the National Science Foundation supercomputer centers. J. Antosiewicz thanks the State Committee for Scientific Research, Poland (grant KBN-4.0078.91.01), for assistance with travel costs Michael K. Gilson is a Howard Hughes Physician Research Fellow. Irwin H. Lee was supported in part by the SMART program of the Baylor College of Medicine and the Keck Center for Computational Biology.

REFERENCES

Antosiewicz, J., M. K. Gilson, and J. A. McCammon. 1994a. Acetylcholinesterase: Effects of ionic strength and dimerization on the rate constants. *Israel. J. Chem.* 34:151–158.

Antosiewicz, J., J. A. McCammon, and M. K. Gilson. 1994b. Prediction of pH-dependent properties of proteins. *J. Mol. Biol.* 238:415–436.

Antosiewicz, J., and D. Porschke. 1988. Turn of promotor DNA by cAMP receptor protein characterized by bead model simulation of rotational diffusion. *J. Biomol. Struct. Dyn.* 5:819–837.

Barnard, E. A. 1974. Enzymatic destruction of acetylcholine. *In* The Peripheral Nervous System. J. I. Hubbard, editor. Plenum Press, New York.

Bazelyansky, M., E. Robey, and J. F. Kirsch. 1986. Fractional diffusion-limited component of reactions catalyzed by acetylcholinesterase, *Biochemistry.* 25:125–130.

Berman, H. A., K. Leonard, and M. W. Nowak. 1991. Function of the peripheral anionic site of acetylcholinesterase. *In* Cholinesterases: Structure, Function, Mechanism, Genetics and Cell Biology. J. Massoulie, F. Bacou, E. Barnard, A. Chatonnet, B. P. Doctor, and D. M. Quinn, editors. American Chemical Society, Washington, D.C., 229–234.

Brooks B. R., R. E. Bruccoleri, B. D. Olafson, D. J. States, S. Swaminathan, and M. Karplus. 1982. CHARMm: a program for macromolecular energy, minimization and dynamics calculations, *J. Comput. Chem.* 4:187–217.

Cantor, C. R., and P. R. Schimmel. 1980. Biophysical Chemistry, Vol. 2. W. H. Freeman and Co., San Francisco.

Davis, M. E., J. D. Madura, B. A. Luty, and J. A. McCammon. 1991. Electrostatics and diffusion of molecules in solution: simulations with the University of Houston Brownian Dynamics program. *Comput. Phys. Commun.* 62:187–197.

Einstein, A. 1905. Uber die von der molekularkinetischen theorie der wärme geforderte bewegung von in ruhenden flüssigkeiten suspendierten teilchen, *Ann. Physik* 17:549–560.

Ermak, D. L. and J. A. McCammon. 1978. Brownian dynamics with hydrodynamic interactions, *J. Chem. Phys.* 69:1352–1360.

Fersht, A. 1985. Enzyme Structure and Mechanism, 2nd ed. W. H. Freeman and Co., San Francisco.

Garcia de la Torre, J. and V. A. Bloomfield. 1981. Hydrodynamic properties of complex, rigid, biological macromolecules: theory and applications, *Q. Rev. Biophys.* 14:81–139.

Gilson, M. K. 1993. Multiple-site titration and molecular modelling: two rapid methods for computing energies and forces for ionizable groups in proteins. *Proteins: Struct. Funct. Gen.* 15:266–282.

Gilson, M. K. and B. H. Honig. 1986. The dielectric constant of a folded protein, *Biopolymers.* 25:2097–2119.

Gilson, M. K., K. A. Sharp, and B. H. Honig. 1988. Calculating the electrostatic potential of molecules in solution: method and error assessment. *J. Comput. Chem.* 9:327–335.

Gilson, M. K., T. P. Straatsma, J. A. McCammon, D. R. Ripoll, C. H. Faerman, P. H. Axelsen, I. Silman, and J. L. Sussman. 1994. Open "back door" in a molecular dynamics simulation of acetylcholinesterase, *Science* 253:1276–1278.

Harel, M., I. Schalk, L. Ehret-Sabatier, F. Bouet, M. Goeldner, C. Hirth, P. Axelsen, I. Silman, and J. L. Sussman. 1993. Quaternary ligand binding to aromatic residues in the active-site gorge of acetylcholinesterase, *Proc. Natl. Acad. Sci. USA.* 90:9031.

Jorgensen, W. L., and J. Tirado-Rives. 1988. The OPLS potential function for proteins: energy minimizations for crystals of cyclic peptides and crambin, *J. Am. Chem. Soc.* 110:1657–1666.

Klapper, I., R. Hagstrom, R. Fine, K. Sharp, and B. Honig. 1986. Focusing of electric fields in the active site of Cu,Zn superoxide dismutase, *Proteins: Struct. Func. Gen.* 1:47–79.

Luty, B. A., S. El-Amrani, and J. A. McCammon. 1993a. Simulation of the bimolecular reaction between superoxide and superoxide dismutase: synthesis of the encounter and reaction steps, *J. Am. Chem. Soc.* 115: 11874–11877.

Luty, B. A., R. C. Wade, J. D. Madura, M. E. Davis, J. M. Briggs, and J. A. McCammon. 1993b. Brownian dynamics simulations of diffusional encounters between triose phosphate isomerase and glyceraldehyde phosphate: electrostatic steering of glyceraldehyde phosphate, *J. Phys. Chem.* 97:233–237.

Madura, J. D., M. E. Davis, M. K. Gilson, R. C. Wade, B. A. Luty, and J. A. McCammon. 1994. Biological applications of electrostatic calculations and Brownian dynamics simulations. *Rev. Comput. Chem.* 5:229–267.

McCammon, J. A., S. H. Norhtrup, and S. A. Allison. 1986. Diffusional dynamics of ligand-receptor association, *J. Phys. Chem.* 90:3901–3905.

Molecular Simulations Inc. 1992. Polar hydrogen parameter set for CHARMm Version 22. Waltham, MA.

Pop, E., M. E. Brewster, J. J. Kaminski, and N. Bodor. 1989. Theoretical study of some heterocyclic amines with applications to the chemistry of 9-amino-1,2,3,4-tetrahydroacridine, *Int. J. Quant. Chem.* 35:315–324.

Radić, Z., G. Gibney, S. Kawamoto, K. MacPhee-Quigley, C. Bongiorno, and P. Taylor. 1992. Expression of recombinant acetylcholinesterase in a baculovirus system: kinetic properties of glutamate 199 mutants, *Biochemistry* 31:9760–9767.

Richards, F. M. 1977. Areas, volumes, packing and protein structure., *Annu. Rev. Biophys. Bioeng.* 6:151–176.

Sines, J. J., S. A. Allison, and J. A. McCammon. 1990. Point charge distributions and electrostatic steering in enzyme/substrate encounter: Brownian dynamics of modified copper/zinc superoxide dismutase, *Biochemistry* 29:9403–9412.

Stryer, L. 1981. Biochemistry, 2nd ed. W. H. Freeman and Co., San Francisco.

Wade, R. C., B. A. Luty, E. Demchuk, J. D. Madura, M. E. Davis, J. M. Briggs, and J. A. McCammon. 1994. Simulation of enzyme-substrate encounter with gated active sites. *Nat. Struct. Biol.* 1:65–69.